Available online at

ScienceDirect
www.sciencedirect.com

Elsevier Masson France
EM|consulte
www.em-consulte.com/en

Original article

Molecular docking study, synthesis and biological evaluation of Schiff bases as Hsp90 inhibitors

Sayan Dutta Gupta [a,c,*], D. Snigdha [a], Gisela I. Mazaira [d], Mario D. Galigniana [d,e], C.V.S. Subrahmanyam [a], N.L. Gowrishankar [b], N.M. Raghavendra [a]

[a] Department of Pharmaceutical Chemistry, Gokaraju Rangaraju College of Pharmacy, Osmania University, Bachupally, Hyderabad, India
[b] Swami Vivekananda Institute of Pharmaceutical Sciences, Nalgonda, Andhrapradesh, India
[c] R&D centre, Department of Pharmaceutical Sciences, Jawaharlal Nehru Technological University, Hyderabad, India
[d] Department of Biological Chemistry, Faculty of Natural Sciences, University of Buenos Aires, Buenos Aires, Argentina
[e] Institute of Experimental Biology and Medicine-CONICET, Buenos Aires, Argentina

A R T I C L E I N F O

A B S T R A C T

Heat shock protein 90 (Hsp90) is an emerging attractive target for the discovery of novel cancer therapeutic agents. Docking methods are powerful *in silico* tools for lead generation and optimization. In our mission to rationally develop novel effective small molecules against Hsp90, we predicted the potency of our designed compounds by Sybyl surflex Geom X docking method. The results of the above studies revealed that Schiff bases derived from 2,4-dihydroxy benzaldehyde/5-chloro-2,4-dihydroxy benzaldehyde demonstrated effective binding with the protein. Subsequently, a few of them were synthesized (1–10) and characterized by IR, ^{1}HNMR and mass spectral analysis. The synthesized molecules were evaluated for their potential to suppress Hsp90 ATPase activity by Malachite green assay. The anticancer studies were performed by 3-(4,5-dimethythiazol-2-yl)-2,5-diphenyl tetrazolium bromide (MTT) assay method. The software generated results was in satisfactory agreement with the evaluated biological activity.

1. Introduction

Heat shock protein 90 (Hsp90) is a type of molecular chaperone that plays a crucial role in the repair of diverse range of "client" proteins (defined as proteins whose level declines upon treatment with Hsp90 inhibitor) involved in the development and progression of malignancy [1,2]. Therefore, compounds with an ability to attenuate Hsp90 function is considered to be broad spectrum in activity with reduced liability for acquired drug resistance [3]. The function of Hsp90 is driven by hydrolysis of ATP to ADP in the N-terminal domain of the protein followed by ATP/ADP exchange. Blocking of this ATPase activity will lead to cessation of Hsp90 function [4,5]. Hence, majority of Hsp90 inhibitors developed so far competitively dock to the N-terminal ATP binding pocket of the protein [6].

The resorcinol moiety was found to be involved in prominent hydrogen bonding and hydrophobic interactions with the amino acid side chain belonging to the N-terminal ATP binding cleft of

Hsp90 [7–9]. This was reflected in the SAR study of various compounds tested for Hsp90 suppression potential wherein analogues without the two hydroxyl groups were much less potent in the binding assay [10–12]. Moreover, the resorcinol scaffold is suggested to be devoid of any toxic side effects commonly associated with other fragments like quinone, halopyrimidine, etc. [13]. Literature review on anticancer agents revealed that Schiff bases (imines or azomethines) possess cytotoxic properties with no concrete evidence of their mechanism of destroying the cancer cells [14–22]. Studies further indicated that the aldehyde substituent of azomethines were superior to the amine portion in exhibiting cytotoxic effects [23]. Furthermore more recently, two imines used as a precursor for azetdine ring synthesis have been reported to moderately diminish Hsp90 activity [24]. In view of the fact that dihydroxy phenyl group is an established template for Hsp90 inhibition and considering the significant anticancer activity displayed by imines, we performed docking studies of a series of Schiff bases of 2,4-dihydroxy benzaldehyde and 5-chloro-2,4-dihydroxy benzaldehyde derivatives (Fig. 1). The ligands, which fared well in the docking program were synthesized and characterized by IR, ^{1}HNMR and mass spectroscopic studies. A colorimetric assay (malachite green assay) was used to measure the extent of Hsp90 ATPase activity inhibition by our synthesized compounds. This assay determines the amount of free phosphate liberated due to

* Corresponding author. Department of Pharmaceutical Chemistry, Gokaraju Rangaraju College of Pharmacy, Osmania University, Bachupally, Hyderabad, India. Tel.: +91 40 3291 2927; fax: +91 40 2304 0860.
E-mail addresses: sayandg@rediffmail.com, sayanduttagupta1@rediffmail.com (S. Dutta Gupta).
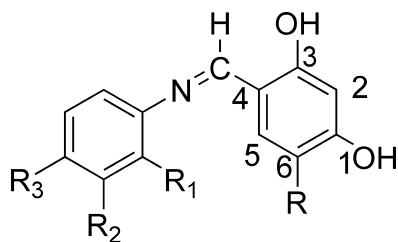
Fig. 1. General structure of Schiff bases synthesized with numbering system used in this report.

ATP hydrolysis and is based on the reaction of phosphomolybdate complex with malachite green. The synthesized molecules were further screened for cytotoxic activity on PC3 prostate cancer cells. The results of the above studies are presented in this paper.

2. Materials and methods

2.1. Molecular docking studies

The docking studies was carried out with Surflex Geom X programme of Sybyl X-1.2 version softwares installed on Dell Precision T-1500 workstation [Intel(R) Core(TM) i7 CPU 860 @ 2.80 GHz 2.79 GHz; 12.0 GB RAM, 1 TB Hard disk]. Crystal structure of Hsp90 was selected from the Protein Data Bank (PDB ID: 3EKR) with a resolution of 2Å [25]. The protein preparation step involved addition of hydrogen and removal of water molecules except 902, 903, 981 and 1026 [26,27]. These four water molecules were revealed to be important for effective ligand-protein binding [27–31]. The protein was energy minimized using conjugate minimization technique of Powell [32]. The protomol (idealized active site) was generated from hydrogen-containing protein mol2 file by keeping the default parameters (threshold factor of 0.5Å and a bloat of 0Å) [33,34]. The ligands were first drawn in Chem draw, saved as mol files and then converted into SD file format by using Schrodinger software (Maestro, 9.1 versions). The ligands were then prepared for docking by first generating a clean 3D conformation using Concord program which generates 20 conformations per structure [32,35]. This is followed by filtering structures based on drug-likeness and docking them with the prepared protein at the developed protomol [36].

2.2. Synthesis of compounds

The chemicals, reagents and solvents employed for synthesis were procured from Hi-media Laboratories Private Limited, Merck specialties Private Limited and SD fine-chem limited. The progress of the reaction and purity was monitored by using TLC Silica gel 60 F_{254} aluminium sheets (Merck F_{254}, Darmstadt, Germany) developed in mobile phase containing ethyl acetate and petroleum ether (1:1). The melting point of the synthesized compounds was determined by DRK Digital melting point apparatus. IR spectra were recorded on Shimadzu IR-Affinity spectrometer using KBr pellets. The ^{1}HNMR spectra of the compounds synthesized were acquired in deuterated DMSO on a Bruker ARX 400/300 MHz (Bruker AG, Fallanden, Switzerland) instrument. Tetramethylsilane was used as the internal standard and all chemical shift values were expressed in parts per million (δ, ppm). The mass spectra were obtained from 6120 Quadrupole LC/MS mass spectrometer using atmospheric pressure-electron spray ionization method (Agilent Technologies, California, USA).

2.2.1. Synthesis of 2,4-dihydroxy benzaldehyde [37]

This was prepared according to a reported procedure (Fig. 2). A two necked round bottom flask was charged with DMF (2.37 mL, 0.0306 mole) and acetonitrile (7 mL). This was followed by addition of $POCl_3$ (2.43 mL, 0.026 mole) drop wise to the reaction mixture by maintaining the temperature between 22 °C to 28 °C. The reaction was stirred at 22–28 °C for 1 h. The solution remains clear throughout. Subsequently the reaction mixture was cooled in a dry-ice bath to −15 to −17 °C and a solution of resorcinol (2.5 g, 0.022 mole) in acetonitrile (7 mL) was slowly added. Precipitation of the Vilsmeier formamidinium phosporodichloridate salt occurs during this addition. The reaction was stirred for an additional 2 h at −15 to −17 °C and then at 28–32 °C for 1 h. The reaction was cooled to 5 °C and after stirring for 1 h the product is isolated by filtration and washed with cold acetonitrile. The intermediate salt was added portion wise to a beaker containing water (62 mL) stirred at 40 °C. The reaction was heated to 52 °C for 0.5 h, and then cooled. When the temperature has reached 35 °C sodium thiosulfate solution (0.09 M, 1 mL) was added to discharge the resulting pink coloration. The reaction was cooled to 5 °C and stirred for 2 h. The mixture was then filtered; the white solid was washed with cold water and air dried for 2 h to obtain a white crystalline solid.

2.2.2. Synthesis of 5-chloro-2,4-dihydroxy benzaldehyde [38]

2, 4-dihydorxy benzaldehyde (3.5 g, 0.0253 mole) was dissolved in 100 mL of water and 24 mL of 4% sodium hydroxide contained in a beaker. This solution is cooled to 20 °C and mixed with 200 mL of sodium hypochlorite solution. The temperature was maintained at 20 °C for 1 hour with occasional stirring. Upon acidifying with HCl a light yellow precipitate of the product was obtained. It was recrystallized from methanol/water to obtain pure crystals of 5-chloro-2,4-dihydroxy benzaldehyde (Fig. 2).

2.2.3. Synthesis of 2,4-Dihydroxy benzaldehyde/5-chloro-2,4-dihydroxy benzaldehyde derived Schiff base derivatives

2,4-dihydroxy benzaldehyde (0.5 g, 0.0036 mole)/5-chloro-2,4-dihydroxy benzaldehyde (0.5 g, .0028 mole) and eqimolar concentration of various aniline derivatives was transferred to a round bottom flask containing absolute ethanol sufficient enough to dissolve the added reagents. The reaction mixture was then refluxed for 3 h (Fig. 2). The TLC was monitored until completion of the reaction. Subsequently water was added resulting in the formation of colored solid, which was filtered and air dried. It was further recrystallized from methanol to obtain the pure product. The general structure of the ligands with the numbering system used in this work is shown on Fig. 1 with detail of the exact structures given in Table 1.

2.3. HSP 90 ATPase inhibitory activity

The plasmid pRSETA encoded His$_6$-tagged human Hsp90β (hHsp90β) was a kind gift from Dr. Chrisostomos Prodromou, University of Sussex, United Kingdom. Expression and purification of the chaperone was achieved as described earlier [5]. ATPase activity was measured following a modification of previously reported procedure [39,40]. Briefly, 10 μg of pure hHsp90β was incubated with the inhibitor to be tested (geldanamycin was used as a standard drug) for 10 min at 20 °C in a buffer containing 50 mM Hepes at pH 7.5, 6 mM MgCl$_2$, 20 mM KCl, and 1 mM ATP. The reaction was stopped by the addition of two volumes of malachite green reactive solution prepared as described by Harder et al. [41]. After 25 min at room temperature, the absorbance at 630 nm was measured [42,43].

2.4. In vitro cell viability assay

The compounds were screened for their cytotoxicity on PC3 prostate cancer cells by adopting the MTT [3-(4, 5-dimethylthiazol-2-yl)-2,5-diphenyl tetrazolium bromide] based cell proliferation assay method [44,45]. The carcinoma cell lines were harvested
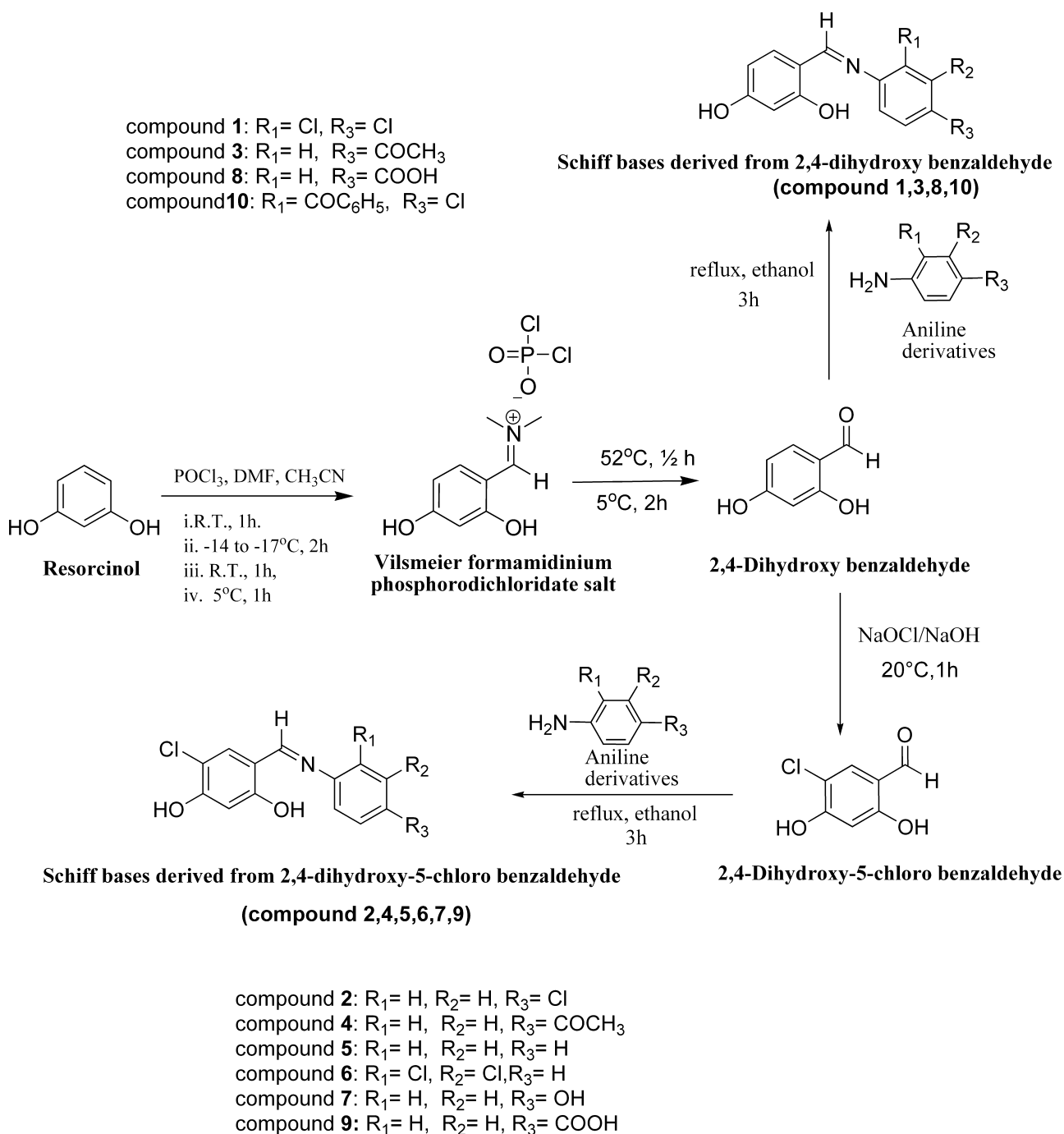
compound **1**: R$_1$= Cl, R$_3$= Cl
compound **3**: R$_1$= H, R$_3$= COCH$_3$
compound **8**: R$_1$= H, R$_3$= COOH
compound**10**: R$_1$= COC$_6$H$_5$, R$_3$= Cl

Schiff bases derived from 2,4-dihydroxy benzaldehyde (compound 1,3,8,10)

reflux, ethanol
3h

Aniline derivatives

POCl$_3$, DMF, CH$_3$CN

i. R.T., 1h.
ii. -14 to -17°C, 2h
iii. R.T., 1h,
iv. 5°C, 1h

Resorcinol

Vilsmeier formamidinium phosphorodichloridate salt

52°C, ½ h
5°C, 2h

2,4-Dihydroxy benzaldehyde

NaOCl/NaOH
20°C, 1h

2,4-Dihydroxy-5-chloro benzaldehyde

Aniline derivatives

reflux, ethanol
3h

Schiff bases derived from 2,4-dihydroxy-5-chloro benzaldehyde

(compound 2,4,5,6,7,9)

compound **2**: R$_1$= H, R$_2$= H, R$_3$= Cl
compound **4**: R$_1$= H, R$_2$= H, R$_3$= COCH$_3$
compound **5**: R$_1$= H, R$_2$= H, R$_3$= H
compound **6**: R$_1$= Cl, R$_2$= Cl, R$_3$= H
compound **7**: R$_1$= H, R$_2$= H, R$_3$= OH
compound **9:** R$_1$= H, R$_2$= H, R$_3$= COOH

Fig. 2. General scheme of synthesis of Schiff bases.

in RPMI1640 (Invitrogen)/10% fetal bovine serum (Gibco) medium supplemented with 0.007% streptomycin and 0.002% penicillin. The cells were then counted and incubated for 37 °C with 5% CO$_2$ in a 96 well microplates. When the cells reach 80% confluence, then the test compounds and standard at concentration was added at concentration ranging from 0.1 μM–5 μM. Cells incubated with vehicle (DMSO) served as a control group. After 48 h incubation, 5 μL of MTT reagent along with 45 mL of phenol red and FBS free DMEM was added to each well and the plates were incubated at 37 °C with 5% CO$_2$ for 4 h. Subsequently, 50 mL of solubilization buffer was added to each well to solubilize the colored formazan crystals produced by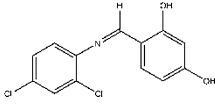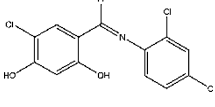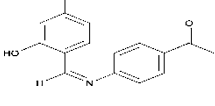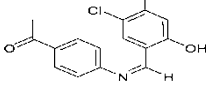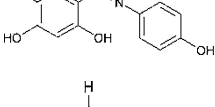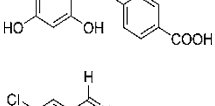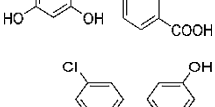 the reduction of MTT. After 48 h, the optical density was measured at 550 nm using spectrophotometer in a microplate reader (Bio-Rad, USA). Geldanamycin was used as standard reference compound [46].
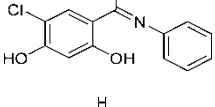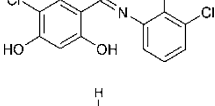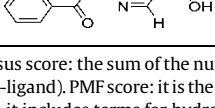
3. Results and discussion

3.1. Molecular docking studies

The docking results revealed that ten compounds (1–10) exhibited good docking score and interacted with amino acids at the N-terminal ATP binding pocket of Hsp90 in a similar fashion. The results of the ligand-protein binding studies are highlighted in

Table 1
Structure and docking results of the synthesized molecules.

Compound	Structure	Total score	Crash	Polar	G score	PMF score	D score	Chem score	C score
1		4.38	−0.87	2.45	−127.66	−12.35	−93.58	−17.83	2
2		4.33	−1.00	2.37	−139.07	−17.64	−101.21	−19.74	2
3		5.03	−0.88	2.40	−102.50	−10.80	−95.976	−18.33	2
4		5.08	−1.19	2.37	−134.02	−13.06	−106.19	−18.50	2
5		4.84	−1.00	2.40	−129.17	−12.80	−98.51	−18.79	2
6		3.82	−0.82	2.40	−129.57	−15.37	−102.34	−18.53	2
7		5.19	−1.17	3.17	−173.18	−15.15	−103.17	−18.376	2
8		4.67	−1.02	2.45	−122.29	−11.24	−97.70	−17.12	2
9		5.23	−2.30	4.52	−181.29	−0.02	−20.19	−18.816	2
10		5.18	−1.06	1.25	−176.37	−11.21	−118.43	−20.69	2

C score: the consensus score: the sum of the number of 'good' results for each ligand in each scoring function. G score: it is based on hydrogen bonding, complex (ligand-protein), and internal (ligand-ligand). PMF score: it is the free energies of interactions for protein-ligand atom pairs. D score: it is based on van der Waals interaction between protein and the ligand. Chem score: it includes terms for hydrogen bonding, metal-ligand interaction, lipophilic contact and rotational entropy, along with an intercept term. Total score: total output of all the scores. Crash: the ability of the compound to penetrate the active site of the protein. Polar: the polar interaction between the ligand and the protein.

Table 1. Our designed molecules formed hydrogen bond contact with Asp 93, Asn 51, Asn 106, Lys 58, Asp 54 and water molecule 902, 903 and 981. The compounds displayed hydrophobic interaction with amino acid Phe 138, Val 186, Ile 91, Met 98, Leu 48, Leu 107, Thr 184, Ala 55, Ile 96, Val 136 and Val 150. The following hydrogen bond interaction was found to be common for all the molecules:

- 2′–OH group with Asn 51 and water molecule 903;
- two hydrogen bond contacts between 4′–OH and Asp 93;
- one hydrogen bond between 4′–OH and water molecule 902 (absent in 2 and 3).

Compound 9 with the highest docking score exhibited the following additional hydrogen bond contacts:

- imine nitrogen with Thr 184 and water molecule 903;
- carboxylic oxygen with Lys 58, Asn 106 and water molecule 981.

Ligand 7, which ranked second in docking analysis formed another hydrogen bond with Asp 54. The binding mode of the 9 is depicted on Fig. 3a and b.

3.2. Synthesis

The series of Schiff bases derived from 2,4-dihydroxy benzaldehyde and 5-chloro 2,4-dihydroxy benzaldehyde were characterized by melting point, R_f values, IR, ^{1}HNMR and mass spectroscopy. All the relevant data regarding characterization of compounds is given Table 2.
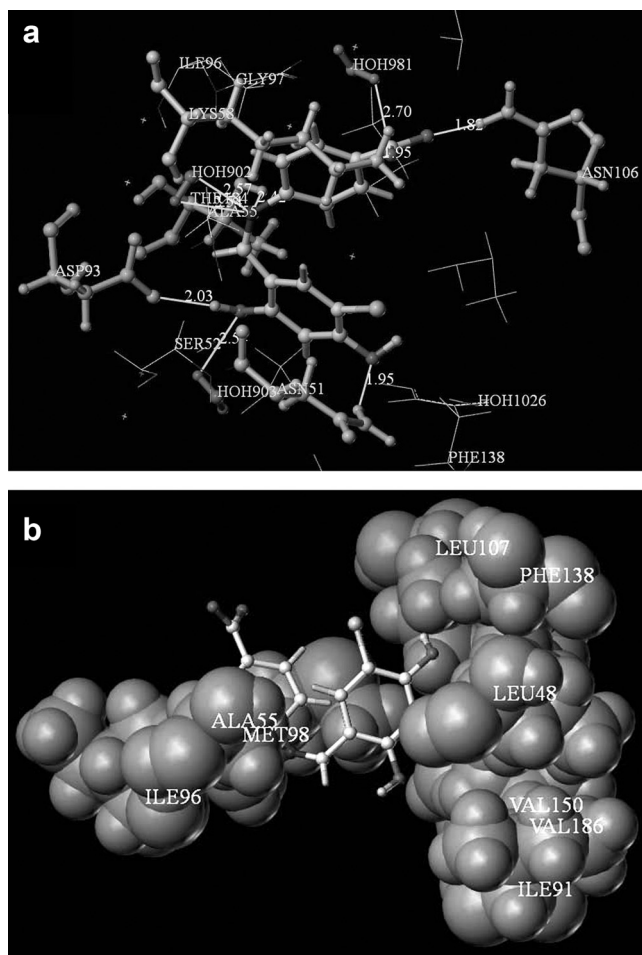
Fig. 3. a: hydrogen bonding interaction (white bold line) of 9 (ball and stick model) with amino acid residue (ball and stick model) and water moleule (ball and stick model) of 3EKR protein; b: hydrophobic contact of ligand 9 (ball and stick model) and HSP 90 protein (PDB ID: 3EKR). The spheres denote hydrophobic amino acids.

The absence of the aldehydic carbonyl stretching bands and the appearance of the characteristic azomethine bands between 1645–1614 cm^{-1} confirmed the formation of the Schiff bases. The broadness of the OH band observed between 3150–3641 cm^{-1} may be attributed to the intramolecular hydrogen bond between CH═N (imine nitrogen) and OH (phenolic) group [21,47]. Medium intensity bands in the range of 1260–1178 cm^{-1} were also observed due to the phenolic C–OH stretching vibrations. The presence of additional bands between 1516 and 1427 cm^{-1} were characteristic of C═C bands of the aromatic rings. The chlorine containing compounds (1,2 and 10) showed corresponding C–Cl stretching bands between 1137–1033 cm^{-1}.

The formation of the ligands by ^{1}HNMR spectroscopy was confirmed by the presence of an azomethine proton signal at 8.8–8.9 and absence of CHO proton signal at 9.8/9.9 assigned to the starting material, 2,4-dihydroxy benzaldehyde/5-chloro 2,4-dihydroxy ben-zaldehyde [24]. The signal corresponding to the 2′-hydroxyl groups was shifted downfield because of intramolecular hydrogen bonding between it and the nitrogen of azomethine (OH–N═C) [48]. In case of S6 where there was no possibility for the OH group to form hydrogen bond, the corresponding signal was shifted to upfield.

The mass spectra of the compounds displayed base peak at M$^+$ and M$^+$+1 corresponding to their respective molecular weight. The chlorine containing ligands exhibited two isotopic peaks at M$^+$ and (M+2)$^+$ peak (percentage abundance ratio: 3:1) due to the isotopes of chlorine.

3.2.1. Vilsmeier formamidinium phosphoro dichloridate salt

IR (KBr cm^{-1}): 3022–2650 (OH, CH, P–OH stretching); 1643 (C═N stretching); 1614, 1583, 1517, 1346 (P═O stretching, free/bonded and C–O stretching); 1109, 1076 (P–O–C stretching); 555, 528, 493 (P–Cl vibration).

3.2.2. 2,4-Dihydroxy benzaldehyde

IR (KBr cm^{-1}): 3103 (OH– stretching); 3037 (C–H aromatic stretching); 2848 (C–H stretching aldehyde); 1628 (C═O stretching, aldehyde); 1496 (C═C aromatic stretching); 1395 (C–H bending aldehyde); 1228 (C–OH stretching). ^{1}HNMR (DMSO, 400 MHz) δ: 10.84 (s, 1H, OH); 10.83 (s, 1H, OH); 9.92 (s, 1H, O═CH); 7.51 (d, 1H, Ar-H, J = 8.8); 6.40 (dd, 1H, Ar-H, ABX; J_{BA} = 8.8 Hz, J_{BX} = 2 Hz); 6.31 (d, 1H, Ar-H, J_{BX} = 2 Hz). Mass (m/z): 137 (M-1)$^-$ (base peak).

3.2.3. 5-chloro-2,4-dihydroxy benzaldehyde

IR (KBr cm^{-1}): 3331 (OH stretching); 3084 (C–H aromatic stretching); 2898 (C–H stretching aldehyde); 1618 (C═O, aldehyde stretching); 1506, 1497 (C═C aromatic stretching); 1228 (C–OH stretching); 1033 (C–Cl stretching). ^{1}HNMR (DMSO, 400 MHz) δ: 11.68 (s, 1H, OH); 11.60 (s, 1H, OH); 9.83 (s, 1H, O═CH); 7.56 (d, 1H, Ar-H, J = 8.8 Hz); 6.69 (d, 1H, Ar-H, J = 8.4 Hz). Mass (m/z): 170.9 (M-1)?.

3.2.4. 4-((2,4-dichlorophenylimino)methyl)benzene-1,3-diol (1)

IR (KBr cm^{-1}): 3650 (OH stretching); 3076 (aromatic C–H stretching); 1614 (C═N stretching); 1504 (C═C aromatic stretching); 1253 (C–OH stretching); 1100 (C–Cl stretching). ^{1}HNMR (DMSO, 400 MHz) δ: 13.34 (s, 1H, OH); 10.42 (s, 1H, OH); 8.87 (s, 1H, imine C–H); 7.61 (s, 1H, Ar-H); 7.51 (d, 1H, Ar-H, J = 2.4 Hz); 7.49 (d, 1H, Ar-H, J = 2.4 Hz); 7.45 (d, 1H, Ar-H, J = 8 Hz); 6.45 (dd, 1H, Ar-H, ABX; J = 8.4 Hz, J = 2.4 Hz); 6.32 (d, 1H, Ar-H, J = 1.6 Hz). Mass (m/z): 280.1 (M-1)?.

Table 2
Physical parameters of the compounds.

Compound	Molecular weight	Melting point (°C)	R_f[a]	% Yield	Color/physical state
1	282	170–172	0.62	65	Dark yellow crystals
2	316	194–196	0.69	59	Light yellow crystals
3	255	181–183	0.57	71	Orange crystals
4	289	170–172	0.69	70	Light orange crystals
5	247	225–228	0.70	57	Greenish yellow crystals
6	316	235–238	0.80	55	Yellow crystals
7	263	200–201	0.50	60	Yellowish green crystals
8	257	179–181	0.40	68	Yellow crystals
9	291	248–251	0.60	40	Reddish orange crystals
10	351	235–238	0.55	55	Yellowish orange crystals

[a] Determined in 50% ethylacetate/petroleum ether solvent system.

Table 3
Biological data for Hsp90 inhibitors[a].

Compound	ATPase activity IC$_{50}$ (μM)	MTT assay IC$_{50}$ (μM)	Compound	ATPase activity IC$_{50}$ (μM)	MTT assay IC$_{50}$ (μM)
1	2.3700	15.3400	7	16.36	10.59
2	0.0003	193.000	8	16.36	93.15
3	0.0004	15.6900	9	0.520	7.999
4	0.0600	16.8000	10	5.000	14.16
5	0.5700	17.7300	Geldanamycin	0.130	2.450
6	59.3400	9.1500			

Hsp90: heat shock protein 90; MTT: 3-(4,5-dimethythiazol- 2-yl)-2,5-diphenyl tetrazolium bromide.
[a] Mean of three independent determinations.

3.2.5. 4-((2,4-dichlorophenylimino)methyl)-6-chlorobenzene-1,3-diol (2)

IR (KBr cm^{-1}): 3625 (OH– stretching); 3095 (aromatic C–H stretching); 1616 (C=N stretching); 1510, 1494 (C=C aromatic stretching); 1255 (C–OH stretching); 1050 (C–Cl stretching). ^{1}HNMR (DMSO, 300 MHz). ^{1}HNMR (DMSO, 300 MHz) δ: 14.51 (s, 1H, OH); 11.20 (s, 1H, OH); 8.93 (s, 1H, imine C–H); 7.64 (s, 1H, Ar-H); 7.51 (d, 1H, Ar-H, J = 2.4 Hz); 7.48 (d, 1H, Ar-H, J = 2.4 Hz); 7.42 (d, 1H, Ar-H, J = 8.6 Hz); 6.64 (d, 1H, Ar-H, J = 8.7 Hz). Mass (m/z): 316.1 (M$^+$).

3.2.6. 4-((4-amino benzophenone) methyl)benzene 1,3 diol (3)

IR (KBr cm^{-1}): 3315 (OH stretching); 3062 (aromatic C–H stretching); 1672 (C=O stretching, ketone); 1633 (C=N stretching); 1508, 1475 (C=C aromatic stretching); 1200 (C–OH stretching); ^{1}HNMR (DMSO, 400 MHz) δ: 13.22 (s, 1H, OH); 10.38 (s, 1H, OH); 8.86 (s, 1H, imine C–H); 8.02 (d, 2H, Ar-H, J = 5.6); 7.46 (m, 3H, Ar-H); 6.43 (d, 1H, Ar-H, J = 6.4 Hz); 6.32 (s, 1H, Ar-H); 2.58 (s, 3H, CH$_3$). Mass (m/z): 256.1 (M+1)$^+$.

3.2.7. 4-((4-amino benzophenone)methyl)6-chlorobenzene-1,3-diol (4)

IR (KBr cm^{-1}): 3641 (OH– stretching); 3059 (aromatic C–H stretching); 1668 (C=O stretching, ketone); 1640 (C=N stretching); 1510 (C=C aromatic stretching); 1253 (C–OH stretching); 1037 (C–Cl stretching). ^{1}HNMR (DMSO, 400 MHz) δ: 14.61 (s, 1H, OH); 11.14 (s, 1H, OH); 8.96 (s, 1H, imine C–H); 8.03–8.05 (m, 2H, Ar-H); 7.39–7.56 (m, 3H, Ar-H, J = 8.8 Hz); 6.58 (d, 1H, Ar-H, J = 8.4 Hz); 2.50 (s, 3H, CH$_3$). Mass (m/z): 288 (M-1)?.

3.2.8. 4-chloro-6-((phenylimino)methyl)benzene-1,3-diol (5)

IR (KBr cm^{-1}): 3600 (OH– stretching); 3037 (aromatic C-H stretching); 1618 (C=N stretching); 1516, 1448 (C=C aromatic stretching); 1257 (C–OH stretching); 1050 (C–Cl stretching). ^{1}HNMR (DMSO, 300 MHz) δ: 14.93 (s, 1H, OH); 11.01 (s, 1H, OH); 8.88 (s, 1H, imine C–H); 7.33–7.47 (m, 4H, Ar-H, J = 8.6 Hz); 7.30 (d, 1H, Ar-H, J = 6 Hz); 7.25–7.28 (m, 1H, Ar-H); 6.53 (d, 1H, Ar-H, J = 8.7 Hz). Mass (m/z): 248.2 (M+1)$^+$.

3.2.9. 4-((2,3-dichlorophenylimino)methyl)-6-chlorobenzene-1,3-diol (6)

IR (KBr cm^{-1}): 3300 (OH– stretching); 3064 (aromatic C–H stretching); 1616 (C=N stretching); 1504 (C=C aromatic stretching); 1257 (C–OH stretching); 1039 (C–Cl stretching). ^{1}HNMR (DMSO, 300 MHz) δ: 14.45 (s, 1H, OH); 11.23 (s, 1H, OH); 8.91 (s, 1H, imine C–H); 7.50–7.59 (m, 2H, Ar-H); 7.39–7.45 (m, 2H, Ar-H); 6.64 (d, 1H, Ar-H, J = 8.7 Hz). Mass (m/z): 316 (M$^+$).

3.2.10. 4-((4-hydroxyphenylimino)methyl)-6-chlorobenzene-1,3-diol (7)

IR (KBr cm^{-1}): 3741 (OH– stretching); 3130 (aromatic C–H stretching); 1616 (C=N stretching); 1514 (C=C aromatic stretching); 1175 (C–OH stretching); 1122 (C–Cl stretching). ^{1}HNMR (DMSO, 400 MHz) δ: 15.18 (s, 1H, OH); 10.82 (s, 1H, OH); 9.64 (s, 1H, OH); 8.80 (s, 1H, imine C–H); 7.31 (d, 1H, Ar-H, J = 4.4 Hz); 7.28–7.32 (m, 3H, Ar-H, J = 5.6 Hz); 6.81–6.85 (m, 2H, Ar-H); 6.51 (d, 1H, Ar-H, J = 8.8 Hz). Mass (m/z): 262.2 (M-1)?.

3.2.11. 4-(dihydroxy benzylidieneamino)benzoic acid (8)

IR (KBr cm^{-1}): 3566 (OH– stretching, acid); 3425 (OH– stretching, phenol); 3020 (aromatic C–H stretching); 1788 (C=O stretching, acid); 1645 (C=N stretching); 1514, 1463 (C=C aromatic stretching); 1178 (C–OH stretching); ^{1}HNMR (DMSO, 400 MHz) δ: 13.2 (s, 1H, COOH); 11.59 (s, 1OH); 10.49 (s, 1OH); 8.85 (s, 1H, imine C–H); 7.98 (d, 2H, Ar-H, J = 8.4 Hz); 7.46 (d, 1H, Ar-H, J = 8.8 Hz); 7.41 (d, 2H, Ar-H, J = 8.4 Hz); 6.41 (dd, 1H, Ar-H, ABX; J = 8.4 Hz, J = 2 Hz); 6.32 (s, 1H, Ar-H). Mass (m/z): 258 (M+1)$^+$.
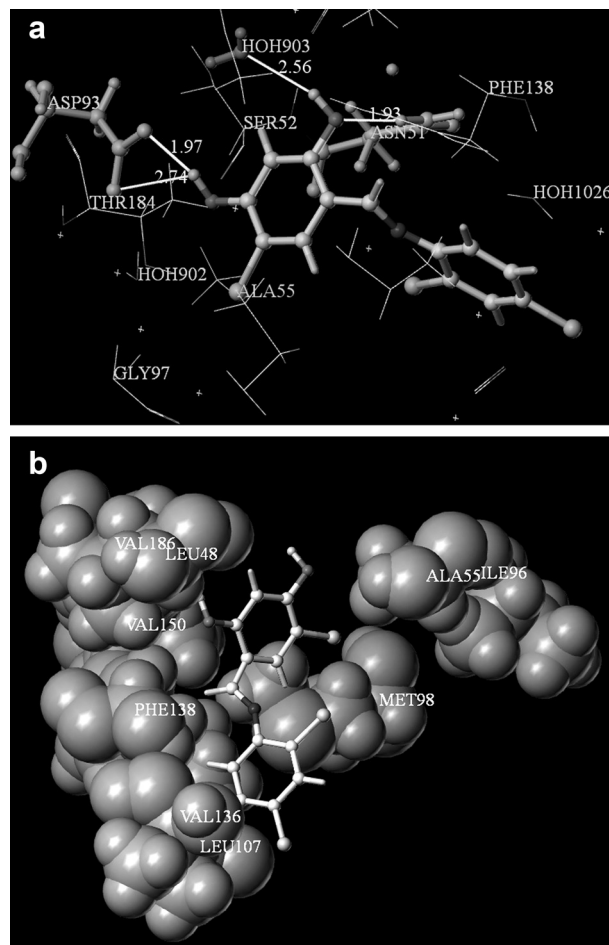
Fig. 4. a: hydrogen bond contact (white bold line) of 2 (ball and stick model) with amino acid residue (ball and stick model) and water molecule (ball and stick model) of 3EKR protein; b: hydrophobic interaction of ligand 2 (ball and stick model) and heat shock protein 90 protein (PDB ID: 3EKR). The spheres indicates hydrophobic amino acids.

Table 4
Predicted cell membrane permeability and partition coefficient[a].

Compound	Caco cell permeability	MDCK cell permeability	Log $P_{o/w}$	Compound	Caco cell permeability	MDCK cell permeability	Log $P_{o/w}$
1	796.268	2067.914	3.13	6	910.633	4350.274	3.475
2	908.924	5231.939	3.55	7	379.655	406.67	1.987
3	349.534	158.824	1.813	8	28.159	13.274	1.544
4	398.296	428.295	2.369	9	32.113	35.828	2.06
5	1150.91	1348.538	3.034	10	741.084	882.759	3.644

Caco cell: cell line derived from human colorectal carcinoma; MDCK cell: Madian-Darby canine kidney epithelial cells; $P_{o/w}$: partition coefficient calculated for n-octanol/water system.
   [a] Schrodinger software's QuickProp programme was employed for these calculations

3.2.12. 4-(5-chloro 2,4- dihydroxy benzylideneamino)benzoic acid (9)

IR (KBr cm^{-1}): 3566 (OH– stretching, acid); 3425 (OH–stretching, phenol); 3150 (aromatic C–H stretching); 1681 (C=O stretching, acid); 1637 (C=N stretching); 1516, 1429 (C=C aromatic stretching); 1197 (C–OH stretching); ^{1}HNMR (DMSO, 300 MHz) δ: 14.60 (s, 1H, COOH); 11.69 (s, 1H, OH); 11.16 (s, 1H, OH); 9.83 (s, 1H, imine C–H); 8.00 (d, 2H, Ar-H, $J = 8.0$ Hz); 7.39 (d, 2H, Ar-H, $J = 8.7$); 6.70 (s, 1H, Ar-H); 6.56 (d, 1H, Ar-H, $J = 6.9$). Mass (m/z): 291 (M-1)?.

3.2.13. 4-((2-benzoyl-4-chlorophenylimino)methyl)benzene-1,3-diol (10)

IR (KBr cm^{-1}): 3641 (OH stretching); 3068 (aromatic C–H stretching); 1680 (C=O stretching); 1629 (C=N stretching imine); 1512, 1469 (C=C aromatic stretching); 1197 (C–OH stretching); 1037 (C–Cl stretching). ^{1}HNMR (DMSO, 300 MHz) δ: 11.11 (s, 1H, OH); 9.83 (s, 1H, OH); 8.83 (s, 1H, imine C–H); 7.77 (s, 1H, Ar-Hz); 7.66–7.75 (m, 1H, Ar-H); 7.52–7.63 (m, 3H, Ar-H); 7.31–7.36 (m, 1H, Ar-H); 7.18 (d, 1H, Ar-H, $J = 6$); 6.92 (d, 2H, Ar-H, $J = 6$); 6.70 (d, 1H, Ar-H, $J = 6$); 6.59 (d, 1H, Ar-H, $J = 6$). Mass (m/z): 350 (M-1)?.

3.3. HSP 90 ATPase inhibitory activity

The primary screening assay (malachite green assay) for evaluating our drug design concept revealed that compound 2 (IC$_{50}$ = 0.0003 μM) and 3 (IC$_{50}$ = 0.0003 μM) are the most potent. None of the other compounds in the series (IC$_{50}$ range from 0.06-59.34) could match the potency of 2 and 3 (Table 3). The compounds, which fared well in docking studies (9 and 7) demonstrated less inhibitory potential than the ones, which scored less (2 and 3). This can be explained from the hydrogen bonding interaction of the molecules in the catalytic site of the protein. 9 and 7 demonstrated good docking results due to more number of hydrogen bond contacts. This has been proved earlier that excess hydrogen bond contact may not lead to increased potency as some of the interactions may be detrimental for activity and may possess agonistic potential. The most active compounds (2 and 3) lack one 'H' bond interaction with water molecule 902 which is present in every molecule (Fig. 4a and b) This proves that binding with water molecule 902 is not beneficial for this series of compounds. This fact was further confirmed from the binding interaction studies of 1 (non-chloro-analogue of 2) and 4 (chloro-analogue of 3). Both 1 and 4 showed only one extra 'H' bond interaction (with water molecule 902), which lead to a significant decrease in their Hsp90 inhibition.

3.4. In vitro cell viability assay

The effects of the synthesized compounds on the growth of PC3 prostate cancer cell lines were tested under in vitro conditions and the results are shown in Table 3. From the Table it is evident that the potencies of the compounds (except 6 and 7) are significantly less in antiproliferative assay compared to the in vitro binding (malachite green) studies. The cell permeability properties of the compounds predicted by QuikProp programme of Schrodinger software was not able to account for the above activity difference (Table 1 and Table 4). This observation may be attributed to multi drug resistance-associated proteins MRP or Glutathione-S-transferase (GST) enzyme, which are overexpressed in PC3 cells and are not clients of Hsp90 [49,50]. Further studies are required to validate the proposed hypothesis. The lack of correlation between the binding affinity of these compounds for Hsp90 and their antiproliferative activity warrants further evaluation of these compounds in other cancer cell lines. However a reverse phenomenon was revealed for 6 and 7. They were found to be less potent in malachite green assay as compared to the MTT assay. Additional studies are necessary to explain the activity difference, but partly could be attributed to their different mechanism of inhibiting the growth of cancer cells.

4. Conclusion

In conclusion we have discovered Schiff bases of 2,4-dihydroxy benzaldehyde/5-chloro-2,4-dihydroxy benzaldehyde as small molecule Hsp90 inhibitors that display potential anticancer activity. This study was guided by structure-based drug design which not only revealed the amino acids (Asp 93, Asn 51 for hydrogen bond interaction; Phe 138, Val 186, Ile 91, Met 98, Leu 48, Leu 107, Thr 184, Ala 55, Ile 96, Val 136 and Val 150 for hydrophobic contact) and water molecule (903) crucial for the protein inhibition but also disclosed the ones not critical for activity (amino acid Thr 184, Lys 58 and water molecule 902). The outcome of the research work will assist in fast and accurate discovery of novel dihydroxy phenyl Schiff base Hsp90 inhibitors with improved efficacy. In future, we plan to design and synthesize more compounds of this series and establish a structure-activity relationship for them.

Disclosure of interest

The authors declare that they have no conflicts of interest concerning this article.

S. Dutta Gupta et al. / Biomedicine & Pharmacotherapy 68 (2014) 369–376

References

[1] Nahleh Z, Tfayli A, Najm A, El Sayed A, Nahle Z. Heat shock proteins in cancer: targeting the "chaperones". Future Med Chem 2012;4:927–35.

[2] Dixit A, Verkhivker GM. Probing molecular mechanisms of the Hsp90 chaperone: biophysical modeling identifies key regulators of functional dynamics. PLoS One 2012;7:e37605.

[3] Martins AS, Davies FE, Workman P. Inhibiting the molecular evolution of cancer through HSP90. Oncotarget 2012;3:1054–6.

[4] Didenko T, Duarte AM, Karagoz GE, Rudiger SG. Hsp90 structure and function studied by NMR spectroscopy. Biochim Biophys Acta 2012;1823:636–47.

[5] Vaughan CK, Piper PW, Pearl LH, Prodromou C. A common conformationally coupled ATPase mechanism for yeast and human cytoplasmic HSP90s. FEBS J 2009;276:199–209.

[6] Neckers L, Trepel JB. Stressing the development of small molecules targeting Hsp90. Clin Cancer Res 2014 [Epub].

[7] Petrikaite V, Matulis D. Binding of natural and synthetic inhibitors to human heat shock protein 90 and their clinical application. Medicina (Kaunas) 2011;47:413–20.

[8] Biamonte MA, Van de Water R, Arndt JW, Scannevin RH, Perret D, Lee WC. Heat shock protein 90: inhibitors in clinical trials. J Med Chem 2010;53:3–17.

[9] Winssinger N, Fontaine JG, Barluenga S. Hsp90 inhibition with resorcyclic acid lactones (RALs). Curr Top Med Chem 2009;9(15):1419–35.

[10] Gopalsamy A, Shi M, Golas J, Vogan E, Jacob J, Johnson M, et al. Discovery of benzisoxazoles as potent inhibitors of chaperone heat shock protein 90. J Med Chem 2008;51:373–5.

[11] Dymock BW, Barril X, Brough PA, Cansfield JE, Massey A, McDonald E, et al. Novel, potent small molecule inhibitors of the molecular chaperone Hsp90 discovered through structure-based design. J Med Chem 2005;48:4212–5.

[12] Verkhivker GM, Dixit A, Morra G, Colombo G. Structural and computational biology of the molecular chaperone Hsp90: from understanding molecular mechanisms to computer-based inhibitor design. Curr Top Med Chem 2009;9:1369–85.

[13] Bolton JL, Trush MA, Penning TM, Dryhurst G, Monks TJ. Role of quinones in toxicology. Chem Res Toxicol 2000;13:135–60.

[14] Tarafder MT, Kasbollah A, Saravanan N, Crouse KA, Ali AM, Tin OK. S-methyl-dithiocarbazate and its Schiff bases: evaluation of bondings and biological properties. J Biochem Mol Biol Biophys 2002;6:85–91.

[15] Guo AJ, Xu XS, Hu YH, Wang MZ, Tan X. Effects of ternary complexes of copper with salicylaldehyde-amino acid Schiff base coordination compounds on the proliferation of BGC823 cells. Chin J Cancer 2010;29:277–82.

[16] Zhao X, Lee PPF, Yan YK, Chu CK. Synthesis, crystal structures and cytotoxicities of some transition metal complexes with N-[2-{(pyridin-2-ylmethylidene)amino}ethyl]acetamide. J Inorg Biochem 2007;101:321–8.

[17] Ganguly A, Chakraborty P, Banerjee K, Choudhuri SK. The role of a Schiff base scaffold, N-(2-hydroxy acetophenone) glycinate-in overcoming multidrug resistance in cancer. Eur J Pharm Sci 2013;14:96–9.

[18] Sztanke K, Maziarka A, Osinka A, Sztanke M. An insight into synthetic Schiff bases revealing antiproliferative activities in vitro. Bioorg Med Chem 2013;21:3648–66.

[19] Li X, Li XQ, Liu HM, Zhou XZ, Shao ZH. Synthesis and evaluation of antitumor activities of novel chiral 1,2,4-triazole Schiff bases bearing gamma-butenolide moiety. Org Med Chem Lett 2012;2:2191–258.

[20] Kumar S, Matharasi DP, Gopi S, Sivakumar S, Narasimhan S. Synthesis of cytotoxic and antioxidant Schiff's base analogs of aloin. J Asian Nat Prod Res 2010;12:360–70.

[21] Creaven BS, Duff B, Egan DA, Kavanagh K, Rosair G, Thangella VR, et al. Anticancer and antifungal activity of copper(II) complexes of quinolin-2(1H)-one-derived Schiff bases. Inorganica Chimica Acta 2010;363:4048–58.

[22] Liu ZC, Wang BD, Yang ZY, Li Y, Qin DD, Li TR. Synthesis, crystal structure, DNA interaction and antioxidant activities of two novel water-soluble Cu2+ complexes derivated from 2-oxo-quinoline-3-carbaldehyde Schiff bases. Eur J Med Chem 2009;44:4477–84.

[23] Hodnett EM, Dunn 3rd WJ. Cobalt derivatives of Schiff bases of aliphatic amines as antitumor agents. J Med Chem 1972;15:339.

[24] O'Boyle NM, Knox AJ, Price TT, Williams DC, Zisterer DM, Lloyd DG, et al. Lead identification of beta-lactam and related imine inhibitors of the molecular chaperone heat shock protein 90. Bioorg Med Chem 2011;19:6055–68.

[25] Kung PP, Funk L, Meng J, Collins M, Zhou JZ, Johnson MC, et al. Dihydroxylphenyl amides as inhibitors of the Hsp90 molecular chaperone. Bioorg Med Chem Lett 2008;18:6273–8.

[26] Jain AN. Surflex-Dock 2.1: robust performance from ligand energetic modeling, ring flexibility, and knowledge-based search. J Comput Aided Mol Des 2007;21:281–6.

[27] de Beer SB, Vermeulen NP, Oostenbrink C. The role of water molecules in computational drug design. Curr Top Med Chem 2010;10:55–66.

[28] Kung PP, Sinnema PJ, Richardson P, Hickey MJ, Gajiwala KS, Wang F, et al. Design strategies to target crystallographic waters applied to the Hsp90 molecular chaperone. Bioorg Med Chem Lett 2011;21:3557–62.

[29] Yan A, Grant GH, Richards WG. Dynamics of conserved waters in human Hsp90: implications for drug design. J R Soc Interface 2008;6:S199–205.

[30] Karpas Z, Eiceman GA, Harden CS, Ewing RG. On the structure of water-alcohol and ammonia-alcohol protonated clusters. J Am Soc Mass Spectrom 1993;4:507–12.

[31] Gupta SD, Subrahmanyam CVS, Raghavendra NM.In: Identification of conserved water molecules and comparative study of docking score in structure-based drug design of HSP 90 inhibitors; 2012.

[32] Wang R, Lu Y, Wang S. Comparative evaluation of 11 scoring functions for molecular docking. J Med Chem 2003;46:2287–303.

[33] Rarey M, Kramer B, Lengauer T. Multiple automatic base selection: protein-ligand docking based on incremental construction without manual intervention. J Comput Aided Mol Des 1997;11:369–84.

[34] Kroemer RT. Structure-based drug design: docking and scoring. Curr Protein Pept Sci 2007;8:312–28.

[35] Wang R, Lu Y, Fang X, Wang S. An extensive test of 14 scoring functions using the PDBbind refined set of 800 protein-ligand complexes. J Chem Inf Comput Sci 2004;44:2114–25.

[36] Cheng T, Li X, Li Y, Liu Z, Wang R. Comparative assessment of scoring functions on a diverse test set. J Chem Inf Model 2009;49:1079–93.

[37] Mendelson WL, Hayden S. Preparation of 2,4-dihydroxybenzaldehyde by the Vilsmeier-Haack reaction. Synth Comm 1996;26:603–10.

[38] Hopkins CY, Chisholm MJ. Chlorination by aqueous sodium hypochlorite. Can J Res 1946;24:208–10.

[39] Scheibel T, Neuhofen S, Weikl T, Mayr C, Reinstein J, Vogel PD, et al. ATP binding properties of human Hsp90. J Biol Chem 1997;272:18608–13.

[40] Rowlands M, McAndrew C, Prodromou C, Pearl L, Kalusa A, Jones K, et al. Detection of the ATPase activity of the molecular chaperones Hsp90 and Hsp72 using the TranscreenerTM ADP assay kit. J Biomol Screen 2010;15:279–86.

[41] Harder KW, Owen P, Wong LK, Aebersold R, Clark-Lewis I, Jirik FR. Characterization and kinetic analysis of the intracellular domain of human protein tyrosine phosphatase beta (HPTP beta) using synthetic phosphopeptides. Biochem J 1994;298:395–401.

[42] Avila C, Kornilayev BA, Blagg BS. Development and optimization of a useful assay for determining Hsp90's inherent ATPase activity. Bioorg Med Chem 2006;14:1134–42.

[43] Rowlands MG, Newbatt YM, Prodromou C, Pearl LH, Workman P, Aherne W. High-throughput screening assay for inhibitors of heat shock protein 90 ATPase activity. Anal Biochem 2004;327:176–83.

[44] Sylvester PW. Optimization of the tetrazolium dye (MTT) colorimetric assay for cellular growth and viability. Methods Mol Biol 2011;716:157–68.

[45] Scudiero DA, Shoemaker RH, Paull KD, Monks A, Tierney S, Nofziger TH, et al. Evaluation of a soluble tetrazolium/formazan assay for cell growth and drug sensitivity in culture using human and other tumor cell lines. Cancer Res 1988;48:4827–33.

[46] Marshall NJ, Goodwin CJ, Holt SJ. A critical assessment of the use of microculture tetrazolium assays to measure cell growth and function. Growth Regul 1995;5:69–84.

[47] Refat MS, El-Deen IM, Ibrahim HK, El-Ghool S. Synthesis and spectroscopic studies of some transition metal complexes of a novel Schiff base ligands derived from 5-phenylazo-salicyladehyde and o-amino benzoic acid. Spectrochim Acta A Mol Biomol Spectrosc 2006;65:1208–20.

[48] Upadhyay KK, Kumar A, Upadhyay S, Mishra PC. Synthesis, characterization, structural optimization using density functional theory and superoxide ion scavenging activity of some Schiff bases. J Mol Struc 2008;873:5–16.

[49] Liu Y, Yan Z, Huang L, Guo M, Zhang Z, Guo C. Cell surface heat shock protein 90 modulates prostate cancer cell adhesion and invasion through the integrin-beta1/focal adhesion kinase/c-Src signaling pathway. Oncol Rep 2011;25:1343–51.

[50] van Brussel JP, van Steenbrugge GJ, Romijn JC, Schroder FH, Mickisch GH. Chemosensity of prostate cancer cell lines and expression of multidrug resistance-related proteins. Eur J Cancer 1999;35:664–71.